Performance analysis of channel coding in satellite communication based on VSAT Network and MC-CDMA scheme

Mohammed El jourmi[1], Hassan El ghazi[2], Abdellatif Bennis[1], Hassan Ouahmane[3]
[1]Physics Department, Hassan II University, FSBM, Casablanca, Morocco
[2]Telecommunications Department, INPT, Rabat, Morocco
[3]Networks and Telecommunications Department, ENSA, El jadida, Morocco
eljourmi.med@gmail.com
elghazi@inpt.ac.ma
al_bennis@yahoo.fr
hassan.ouahmane@yahoo.fr

Abstract: - Satellites are an essential part of our daily life, and they have a very large usage ranging from Search and Rescue Operations to Environmental Monitoring. The widest use of satellites is, however, in communication systems. Satellites can cover vast areas on the world; therefore, they are the nodes where all links pass through in a communications network. Many users can access such a network simultaneously while they are widely separated geographically. The purpose of this paper is to model and analyze a geostationary satellite communication system with VSATs networks in the uplink case, using Multicarrier CDMA system (MC-CDMA is a combination of multicarrier modulation scheme and CDMA concepts) and channel coding mechanisms "Turbo code and Convolutional code". The envisaged system is examined in Ku band and over AWGN channel. The simulation results are obtained for each different case. The performance of the system is given in terms of Bit Error Rate (BER) and Signal to Noise Ratio (SNR). In this study the proposed system coded with Turbo code can achieve better error rate performance compared to coded VSAT MC-CDMA system with convolutional code.

Keywords—VSAT Network, Turbo code, Convolutional code, MC-CDMA, Ku band, Satellite communication, Uplink.

1 Introduction

Communication satellites, and especially in geostationary Earth orbit (GEO), provide an effective platform to relay radio signals between points on the ground. The users who employ these signals enjoy a broad spectrum of telecommunication services on the ground, at sea, and in the air. Benefits of satellite communications should in the 1990's be extended to users in all parts of the world through the use of smaller, inexpensive and less sophisticated Earth stations for two way (voice and data), and one way (video, data) use. Satellite communications pose a major and serious problem when that concerns the presence of random errors on the satellite link and that can significantly degrades the system performance. For this reason we used channel coding mechanisms to reduce the error rate and improve the system performance. The objective of this paper is to design a satellite ground segment component for use in telecommunications and analyze its performance. Therefore, the ground segment is designed to fit in the description of a Very Small Aperture Terminal (VSAT), which requires antenna dimensions less than 1.8 m in diameter. The designed system has a wide bandwidth and use MC-CDMA scheme, BPSK modulation, channel coding (Turbo code and Convolutional code) over AWGN channel. To be able to send signals through great distance, the signals need to be amplified before transmission. The High Power Amplifier (HPA) of Rapp's model which is based on a Solide State Power Amplifier (SSPA) is used and a low noise amplifier (LNA) is used to amplify very weak signals captured by an antenna. In this study, the CDMA encoder uses PN sequences and Walsh Codes to generate a spread signal. Each VSAT uses a different PN sequence and each user in a VSAT uses different Walsh Codes.

This paper is organized as follows. In Section 2 the VSAT Network are briefly described with its configurations. The principle of MC-CDMA scheme is presented with modeling of proposed system in Section 3. Section 4 presents the principle of convolutional coding. The principle of Turbo code is discussed in Section 5. Characteristics of the HPA which is used in this study are illustrated in Section 6. In section 7 the link budget and simulation model

Mohammed El Jourmi, Hassan El Ghazi,
Abdellatif Bennis, Hassan Ouahmane

are presented. Simulation results are presented in Section 8, and conclusions are drawn in Section 9.

2 VSAT Network Configurations

VSAT stands for Very Small Aperture Terminal and it is the term that is normally used to refer to several satellite data communication technologies. The term VSAT assumes the use of a (very) small diameter antenna (terminal) to receive and/or transmit radio signals (data) to/from a satellite [21].

There are two major network configurations viz: the hub-based star VSAT network, which provides a "star" type of topology, and the "mesh" network, which allows connections between any pair of VSATs.

2.1 Meshed VSAT Network

As all the VSATs are visible from the satellite, carriers can be relayed by the satellite from any VSAT to any other VSAT in the network as shown in figure 1. This type of configuration is called point-to-point topology. In this mesh type, earth stations communicate directly via satellite and will have only one hop communication. Regarding the meshed VSAT networks, one must take into account the following limitations [9]:
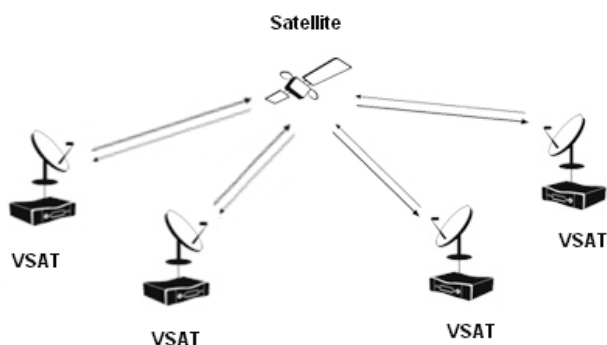

Fig 1. Meshed VSAT Network

- typically 200 dB carrier power attenuation on the uplink and the downlink as a result of the distance to and from a geostationary satellite;
- limited satellite radio frequency power, typically a few tens of watts;
- small size of the VSAT, which limits its transmitted power and its receiving sensitivity.

As a result of the above, it can be noticed that the demodulated signals at the receiving VSAT do not match the quality requested by the user terminals. Therefore direct links from VSAT to VSAT may not be acceptable [13].

2.2 Star-Shaped VSAT Network

When you submit your final version, after your paper has been accepted, prepare it in two-column format, including figures and tables.
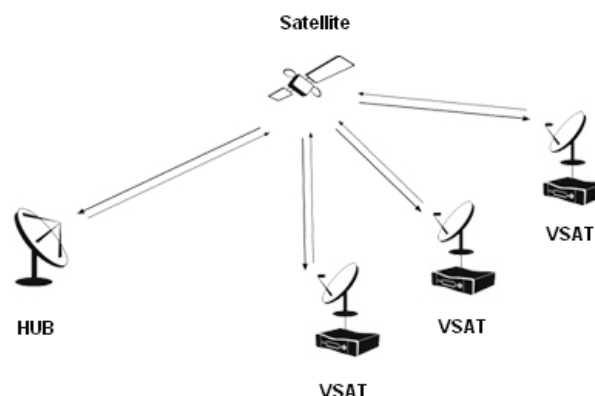

Fig 2. Star-Shaped VSAT Network showing all outbound links

The solution then is to install a station larger than a VSAT in the network, called the hub. The hub station has a larger antenna size than that of a VSAT, about 4m to 11m resulting in a higher gain than that of a typical VSAT antenna, and is equipped with a more powerful transmitter [14]. As a result of its improved capability, the hub station is able to receive adequately all carriers transmitted by the VSATs, and to convey the desired information to all VSATs by means of its own transmitted carriers. The architecture of the network becomes star shaped as shown in figure 2. The links from the hub to the VSAT are named "outbound links" and the ones from the VSAT to the hub are named "inbound links". Both inbound and outbound links consist of two links, uplink and downlink, to and from the satellite.

In conclusion, star shaped networks are imposed by power requirements resulting from the reduced size and hence the low cost of the VSAT earth station in conjunction with power limitation of the satellite. Meshed networks are considered whenever such limitations do not hold, or are unacceptable. Meshed networks have the advantage of a reduced propagation delay (single hop delay is 0.25 sec instead of 0.5 sec for double hop) which is especially of interest for telephone service [11].

3 Multi-Carrier CDMA

Multi-carrier CDMA system is based on a combination of the CDMA scheme and orthogonal frequency division multiplexing (OFDM) signaling. MC-CDMA transmitter spreads the original signal using a given spreading code in the frequency

Mohammed El Jourmi, Hassan El Ghazi,
Abdellatif Bennis, Hassan Ouahmane

domain. In other words, a fraction of the symbol corresponding to a chip of the spreading code is transmitted through a different subcarrier.
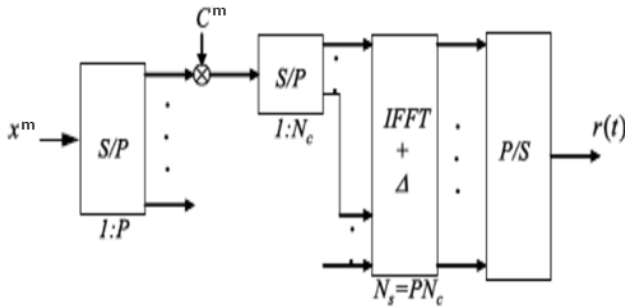

Fig 3. MC-CDMA Transmitter

The figure 3 shows the MC-CDMA transmitter for the mth user. The input information sequence is first converted into P parallel data sequences, and then each Serial/Parallel converter output is multiplied with the spreading code with length L_C. All the data in total $N = P \times L_C$ (corresponding to the total number of subcarriers) are modulated in baseband by the inverse Fast Fourier transform (IFFT) and converted back into serial data. The guard interval Δ is inserted between symbols to avoid intersymbol interference, and finally the signal is transmitted.

Figure 4 shows the MC-CDMA receiver. It requires coherent detection for successful despreading operation and this causes the structure of MC-CDMA receiver to be very complicated. In figure, the k-subcarrier components (k=1,2,…Lc) corresponding to the received data y^m is first coherently detected with FFT and then multiplied with the gain G to combine the energy of the received signal scattered in the frequency domain [7]-[8].
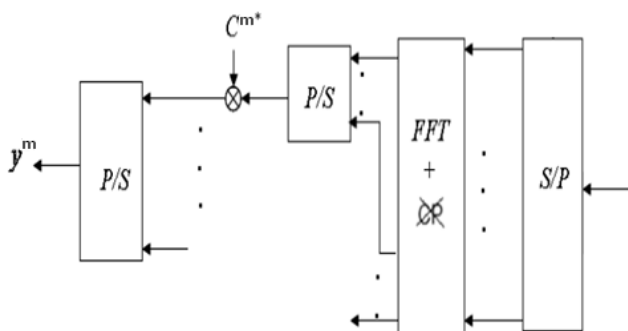

Fig 4. MC-CDMA Receiver

3.1 Transmitter model of envisaged system

Transmitted signal S(t) corresponding to the lth data bit of the mth user is defined by:

$$S(t) = \sqrt{\frac{2P_{\alpha,m}}{N}} \sum_{v=0}^{S-1} \sum_{l=-\infty}^{+\infty} \sum_{n=0}^{N-1} W_{\alpha,m}[n] b_{\alpha,m}[l]$$

$$\cos\left(2\pi\left(f_c + \frac{n}{T_b}\right)t\right) C_\alpha[v] U_{T_b}(t - lT_b)$$

(1)

Where $P_{\alpha,m}$ is the power of data bit, $U_{T_b}(t - lT_b)$ is the rectangular pulse defined in the $[0, T_b]$. Every user has a spreading code $W_{\alpha,m}[n]$ with $n = 0,1,...,N-1$ and N is the length of the sequence chip. The same signature sequence chip is used to modulate each of the N carriers of the mth user. The maximum number of users in the system is M. Every VSAT has a signature $C_\alpha[v]$ with $v = 0,1,...,S-1$ and S is the length of the spreading code. α denote the number of VSATs with $\alpha = 1,2,...,K$ and K is the maximum number of VSATs.

3.2 Receiver model of envisaged system over AWGN

The receiver signal of M active users in the VSAT-MC-CDMA system can be written as:

$$R(t) = \sum_{\alpha=1}^{K} \sum_{v=0}^{S-1} \sum_{m=0}^{M-1} \sum_{l=-\infty}^{+\infty} \sum_{n=0}^{N-1} \sqrt{\frac{2P_{\alpha,m}}{N}} W_{\alpha,m}[n] b_{\alpha,m}[l]$$

$$\cos\left(2\pi\left(f_c + \frac{n}{T_b}\right)t\right) C_\alpha[v] U_{T_b}(t - lT_b)$$

$$+ n(t) + \xi(t)$$

(2)

Where n(t) is the additive white Gaussian noise (AWGN) with double sided power spectral density of $N_0/2$ and $\xi(t)$ is the inter-VSAT interference.

3.3 The Decision Statistic:

The information bits $b_{\beta,j,n}$ received from a user specified (m = j) and VSAT ($\alpha = \beta$) will be used for this analysis. ($\alpha = \beta$) and (m = j) are the indices of despreaded information bits we want to retrieve. All other values of α ($\alpha \neq \beta$) and m (m $\neq$ j) will be considered co-channel interference and inter-VSATs interference.

Assuming that users are synchronous in time, after demodulation and combination of sub-carrier signals, the decision variable is obtained as:

$$\mathcal{Y}_{\beta,j,l} = \frac{1}{T_b} \int_{lT_b}^{(l+1)T_b} R(t) \sum_{n=0}^{N-1} W_{\beta,j}[n]$$
$$\cos\left(2\pi\left(f_c + \frac{n}{T_b}\right)t\right)C_\beta[v]dt \tag{3}$$

The decision variable consists of four components, the first term corresponds to the desired signal, the second term corresponds to the multiple access interference from other users, the third term corresponds to the noise and the last term represents the interference between VSATs.

$$\mathcal{Y}_{\beta,j,l} = \mathcal{D} + \mathcal{MAI} + \eta + \zeta \tag{4}$$

$\mathcal{D}$: Signal désiré

$\mathcal{MAI}$: Interférence Co-canal

η : Bruit blanc gaussien additif

ζ : Interférence entre VSATs

Note that the absence of interference between symbols and the interference between carriers is ensured by the use of a guard interval longer than the delay spread of the channel impulse response.
Components of the decision variable can be written in the following form:

- Desired signal

$$\mathcal{D} = \frac{1}{2}\sqrt{\frac{2P_{\beta,j}}{N}}(S-1)\sum_{l=-\infty}^{+\infty} b_{\beta,j}[1] \tag{5}$$

- Co-channel interference

$$\mathcal{MAI} = \sum_{\substack{m=0 \\ m \neq j}}^{M-1}\sum_{l=-\infty}^{+\infty}\sum_{n=0}^{N-1}\frac{1}{2}\sqrt{\frac{2P_{\beta,m}}{N}}\, b_{\beta,m}[1]$$
$$W_{\beta,m}[n]W_{\beta,j}[n] \tag{6}$$

- Noise

$$\eta = \sum_{v=0}^{S-1}\sum_{n=0}^{N-1}\frac{1}{T_b}\int_{lT_b}^{(l+1)T_b} n(t)\cos\left(2\pi\left(f_c+\frac{n}{T_b}\right)t\right)$$
$$W_{\beta,j}[n]C_\beta[v]dt \tag{7}$$

- Inter-VSATs interference

$$\zeta = \sum_{\substack{\alpha=1 \\ \alpha \neq \beta}}^{K}\sum_{v=0}^{S-1}\sum_{m=0}^{M-1}\sum_{l=-\infty}^{+\infty}\sum_{n=0}^{N-1}\frac{1}{2}\sqrt{\frac{2P_{\alpha,m}}{N}}\, W_{\alpha,m}[n]b_{\alpha,m}[1]$$
$$C_\alpha[v]W_{\beta,j}[n]C_\beta[v] \tag{8}$$

Generally speaking the jth user from the βth earth station, the SNIR can be expressed as:

$$SNIR = \frac{E\left[\left(\mathcal{Y}_{\beta,j}\right)^2\right]}{\sigma\left(\mathcal{Y}_{\beta,j}\right)} \tag{10}$$

Where σ is variance. Assume independent users and independent subcarriers,

$$E\left[\left(\mathcal{Y}_{\beta,j}\right)^2\right] = \frac{1}{4}(S-1)^2\frac{2P_{\beta,j}}{N} \tag{11}$$

$$\sigma\left(\mathcal{Y}_{\beta,j}\right) = \sigma(\eta) + \sigma(\mathcal{MAI}) + \sigma(\zeta) \tag{12}$$
$$\sigma\left(\mathcal{Y}_{\beta,j}\right) = E\left[(\eta)^2\right] + E\left[(\mathcal{MAI})^2\right] + E\left[(\zeta)^2\right] \tag{13}$$

The variance of the noise components is:

$$\sigma(\eta) = \frac{N_0}{4T} \tag{14}$$

The variance of the MAI can be expressed as

$$\sigma(\mathcal{MAI}) = \frac{(N-1)}{4}\sum_{\substack{m=0 \\ m \neq j}}^{M-1}\frac{2P_{\beta,m}}{N} \tag{15}$$

The variance of the inter-VSAT interference is :

$$\sigma(\zeta) = \frac{(N-1)}{4}\sum_{\substack{\alpha=1 \\ \alpha \neq \beta}}^{K}\sum_{m=0}^{M-1}\frac{2P_{\alpha,m}}{N}(S-1) \tag{16}$$

The following expression is the total variance of noise plus interferences of proposed system:

$$\sigma\left(\mathcal{Y}_{\beta,j}\right) = \frac{N_0}{4T} + \frac{(N-1)}{4}\sum_{\substack{m=0 \\ m \neq j}}^{M-1}\frac{2P_{\beta,m}}{N}$$
$$+\frac{(N-1)}{4}\sum_{\substack{\alpha=1 \\ \alpha \neq \beta}}^{K}\sum_{m=0}^{M-1}\frac{2P_{\alpha,m}}{N}(S-1) \tag{17}$$

4 Convolutional coding

A convolutional encoder generates code symbols for transmission utilizing a sequential finite-state machine driven by the information sequence. Decoding these codes then amounts to sequentially observing a corrupted version of the output of this system and attempting to infer the input sequence. From a formal perspective, there is no need to divide the message into segments of some specific length.

Figure 5 illustrates one of the simplest nontrivial convolutional encoders. It is implemented by a shift register of memory (number of delay elements) $m = 2$ and three summers $\oplus$ over Galois field GF(2). The rate of the code is $r = 1/2$. The information sequence $\ldots \beta_0, \beta_1, \ldots, \beta_n \ldots, \beta_n \in \{0, 1\}$, is the input sequence of the encoder. The encoder is a finite-state machine that can be described in terms of its state transition diagram. This is shown in Figure 6, where the nodes refer to the contents of the register just before the next input bit arrives. The encoder inputs $\ldots \beta_0, \beta_1, \ldots, \beta_n, \ldots$, and outputs $\ldots \alpha_0, \alpha_1, \ldots, \alpha_n, \ldots, \beta_n, \alpha_n \in \{0, 1\}$ (2 output symbols per input bit for the rate $r = 1/2$ encoder) are shown as labels on the transition branches[6].
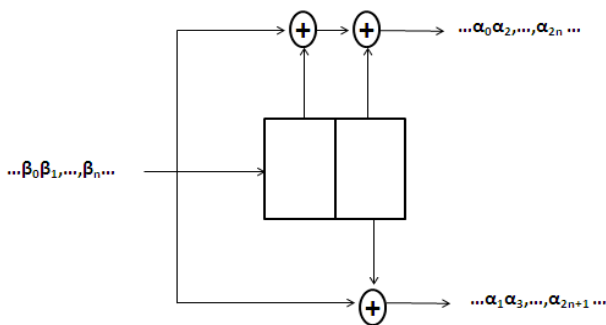

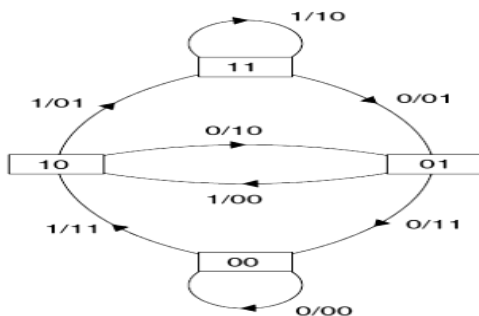Fig. 5 A rate $r = 1/2$ memory $m = 2$ convolutional encoder

Fig. 6 The state-transition diagram for the encoder in Fig. 5

Decoding of convolutional codes is a more difficult problem than encoding. The function of a convolutional decoder is estimating the encoded input information using a method that results in the minimum possible number of errors. Unlike a block code, a convolutional code is a finite state machine. Therefore, the output decoder is a "maximum likelihood estimator" and optimum decoding is done by searching through the trellis for the most probable sequence. Depending on whether hard decision or soft decision decoding is used, either the Hamming or Euclidian metric is used, respectively. Convolutional coding can be decoded with several different algorithms. The Viterbi algorithm is the most commonly used [5], and for this reason we adopted the Viterbi decoder to decode the data encoded with Convolutional encoder.

5 Turbo Coding

Parallel-concatenated convolutional codes (PCCCs), also known as turbo codes, were first introduced by Berrou, Galvieux and Thitimajshima in 1993 [23] and have been shown to offer near-capacity performance for large block sizes. This turbo code is constructed by parallel concatenation of two or more convolutional constituent codes with an interleaver. Encoder and decoder for rate 1/3 turbo code are illustrated in Fig.7 and Fig.8.

One of the key advantages of turbo codes is that they can be decoded by a practical decoding scheme for which the decoding complexity only grows linearly in the length of the code. In general, the complexity of maximum-likelihood (ML) decoding grows exponentially in the length of the code.

5.1 Turbo encoder

In Figure 7 the turbo encoder consists of two convolutional encoders and an interleaver and it produces a recursive Parallel Concatenated Convolutional Code (PCCC). Here the first constituent encoder receives input bits directly, whereas the second constituent encoder is fed with input bits through the interleaver. Furthermore the figure shows that the entire turbo encoder is an 1/3 rate encoder, thus for each input, three outputs are generated. This rate is however altered depending on possible puncturing of bits and tail bits from the second constituent encoder at termination [22].
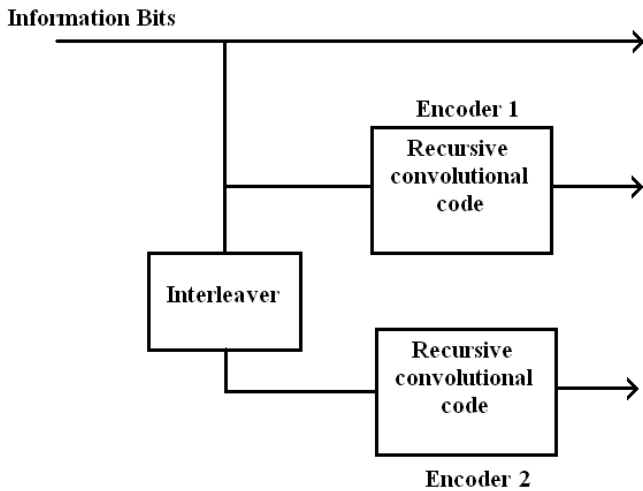
Fig 7. A rate 1/3 Turbo code encoder

5.2 Turbo decoder

The job of the turbo decoder is to reestablish the transmitted data from the received systematic bitstream and the two parity check bitstreams, even though these are corrupted by noise.
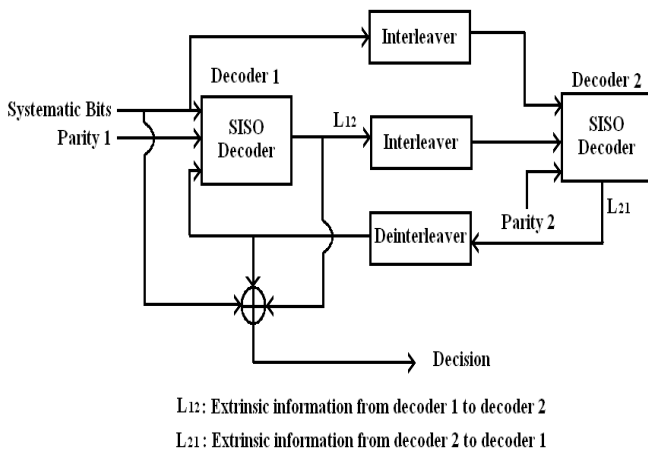

L_{12}: Extrinsic information from decoder 1 to decoder 2

L_{21}: Extrinsic information from decoder 2 to decoder 1

Fig 8. A rate 1/3 Turbo code decoder

In a typical turbo decoding system (see Fig.8), two decoders operate iteratively and pass their decisions to each other after each iteration. These decoders should produce soft-outputs to improve the decoding performance. Such a decoder is called a Soft-Input Soft-Output (SISO) decoder [24]. Each decoder operates not only on its own input but also on the other decoder's incompletely decoded output. In this paper the two SISO decoders used for turbo decoding are Max-Log-Map.

6 High Power Amplifier Model

Power amplifiers are typically the most power-hungry components of RF transceivers. The design of PAs, especially for linear, low-voltage operations, remains a difficult problem defying an

elegant solution. Two type's amplifiers are mostly used in satellite communication: Traveling Wave Tube Amplifier (TWTA) and Solid State Power Amplifier (SSPA). TWTA is mostly used for high power satellite transmitters while SSPA is used in many other applications including small size transmitters as VSAT.

The complex output of RF with non-linear distortion can be expressed as:

$$z(t) = f[u_y(t)]e^{-j[\alpha_y(t)+\phi(u_y(t))]} \qquad (18)$$

Where $u_y(t)$ and $\alpha_y(t)$ are the modulus and phase of the input signal. The measured AM/AM and AM/PM for SSPA is well presented by Rapp's model [16] [15] as:

$$f[u_y] = \frac{u_y}{[1+(u_y/A_{max})^{2P}]^{1/2P}}$$

$$\phi[u_y] = 0 \qquad (19)$$

Here A_{max} is the maximum output amplitude and the parameter p controls the smoothness of the transition from the linear region to the limiting region [15].

For these types of amplifiers we can notice that the SSPA adds no phase distortion.
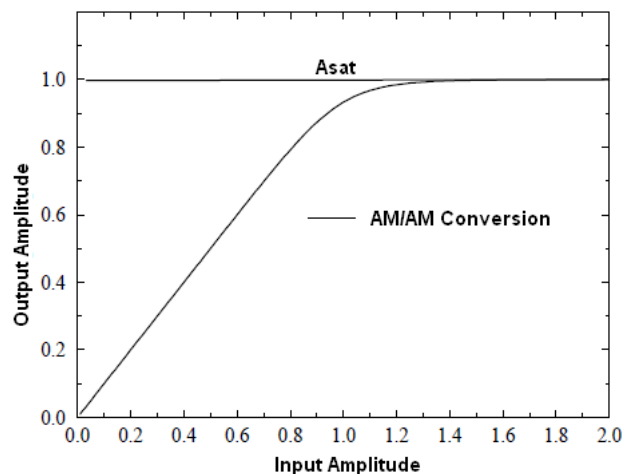

Fig 9. The SSPA characteristics : Normalized AM/AM conversion ($A_{sat}=1$)

The effect of the nonlinear amplifier depends on the operating point, which position is defined by its back-off. Input back-off (IBO) and output back-off (OBO) are two common parameters to specify the nonlinear distortion. IBO corresponds to the ratio

between the saturated and average input power, and is defined as:

$$IBO = 10log10\frac{P_{in,sat}}{P_{in}}, [dB] \qquad (20)$$

and OBO corresponds to the ratio between the saturated and average output power, defined as:

$$OBO = 10log10\frac{P_{out,sat}}{P_{out}}, [dB] \qquad (21)$$
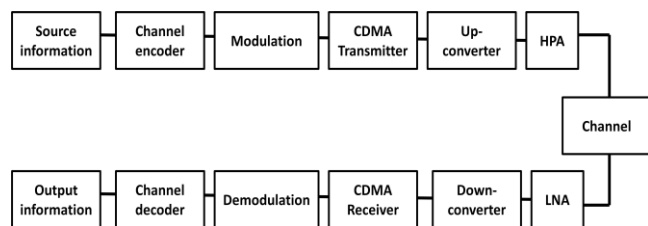
7 Simulation model and System Specification

Fig. 10 Overall Simulation Block Diagram

Figure 10 illustrates the overall simulation model. Binary input signal to the system is converted to symbol stream after passing through the encoder. The frequency domain spreading is done by using signature sequence of length 32 in the CDMA transmitter. Up-converter is capable of outputting its carrier at the desired RF frequency. Signal is amplified with HPA before being transmitted through the transmission channel. LNA amplify very weak signals captured by the VSAT antenna. Down-converter converts the desired signal band to a convenient IF frequency for digitization. Despreading in the CDMA receiver, demodulation is done before passing through the decoder. The original binary data is recovered after passing through the decoder. The parameters that we use in our simulation are as follows:

Table 1: General information

Satellite orbit radius	42242 km
Earth radius	6370 km
Distance from the VSAT to satellite	38054 km
Free space loss	206.1 dB
Speed of light, c	3.108 ms^{-1}
Boltzmann's constant	-228.6 dBJK^{-1} (=1.38×10^{-23}J/K)

Table 2: VSAT Parameters

up-link frequency F_u	14.25 GHz

VSAT HPA output power P_{TxVSAT}	1 W
Antenna diameter	1.2 m
Antenna gain	42.84 dBi
EIRP	42.84 dBW
VSAT latitude	45.5° N
VSAT longitude	9.5° E
Elevation angle	37.56°
Azimuth angle	183.5°
Bit rate R_b	64 kbit/s
Bit rate R_s	128 kbit/s (R_s=R_b/[(1/2 FEC)*(1 bit/symbole)])
Required bandwidth BW_R (1/2 FEC)	168,96 KHz (BW_R=R_s*1,32)

Table 3: Satellite Parameters

Satellite figure of merit $(G/T)_{SL}$	1 dB/K
satellite receiver effective input noise temperature	500 K
Satellite antenna noise temperature	290 K
uplink system noise temperature	790 K
Power Flux density φ	-119.22 dBW/m^2
Transponder bandwidth	54 MHz
Satellite antenna gain	31 dBi
Sub-satellite point longitude	7° E
C/N_0 in up-link	66.34 dBHz

The figure 11 shows the variation of the free space loss (FSL) which depends on the frequency f and on the distance R between the earth station and the satellite [13][9]:

$$L_{FS} = \left(\frac{4\pi Rf}{c}\right)^2 = \left(\frac{4\pi R_0 f}{c}\right)^2 \left(\frac{R}{R_0}\right)^2 \qquad (22)$$

$$L_{FS}(dB) = 10log\left(\frac{4\pi Rf}{c}\right)^2 + 10log\left(\frac{R}{R_0}\right)^2 \qquad (23)$$

Where c is the speed of light ($c = 3 \times 10^8$ ms^{-1}) and R_0 is the satellite height ($R_0 = 35\,786$ Km for a geostationary satellite).

Mohammed El Jourmi, Hassan El Ghazi, Abdellatif Bennis, Hassan Ouahmane
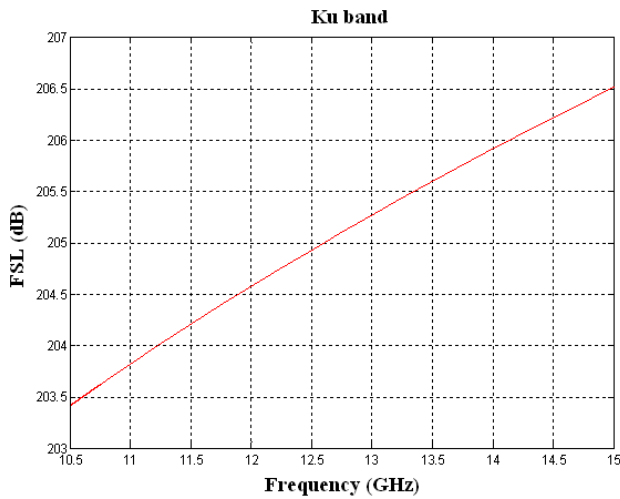

Fig.11 Variation in dB of FSL in Ku band and geostationary satellite

The figure 12 shows the variation of Effective Isotropic Radiated Power (EIRP) of the earth station which depends on the power fed to the transmitting antenna P_T and the earth station antenna transmit gain G_T in the pertinent direction. The EIRP is expressed as:

$$EIRP(W) = P_T G_T \qquad (24)$$

$$EIRP(dBW) = P_T(dBW) + G_T(dBi) \qquad (25)$$

Fig.12 Variation in dBW of EIRP for an antenna diameter =1.2 m and Antenna gain = 42.84

The maximum antenna gain G_{max} of the earth station which depends on the frequency, the antenna efficiency and the antenna diameter is expressed as:

$$G_{max} = \eta_a \left(\frac{\pi D f}{c} \right)^2 \qquad (26)$$

$$G_{max}(dBi) = 10 log \left(\eta_a \left(\frac{\pi D f}{c} \right)^2 \right) \qquad (27)$$

η_a : Antenna efficiency (typically 0.6)

D : Antenna diameter (m)

f : Frequency (Hz)

c : Speed of light (ms^{-1})

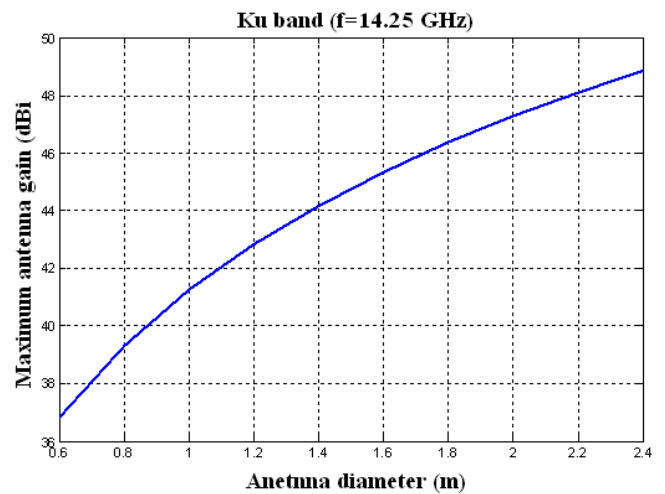Figure 13 display values of these parameters for typical VSAT antenna diameters.

Fig.13 Antenna gain for typical VSAT station antenna diameters

8 RESULTS AND DISCUSSION

In this simulation the performance results of VSAT MC-CDMA system are obtained for uncoded system, coded system with Convolutional code and coded system with Turbo code by using Binary Phase Shift Keying modulation over AWGN channel. In this simulation the number of carriers equals the number of chips of the spreading code, the maximum number of users is 32 users (full loading) and the code length of spreading code is 32 chips.

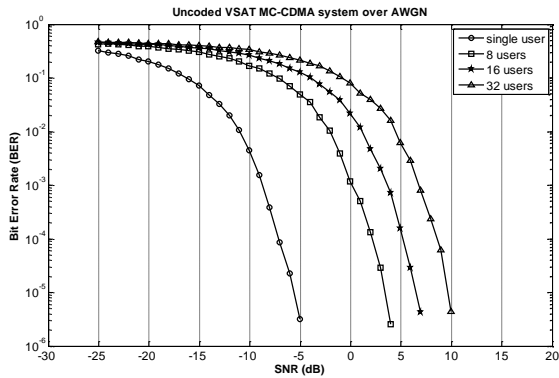## 8.1 Performance of uncoded VSAT MC-CDMA system

Fig.14 Performance of uncoded VSAT MC-CDMA system (for single, 8, 16 and 32 users)

Figure 14 shows the performance of VSAT MC-CDMA system over AWGN channel for single, 8, 16 and 32 users. For different number of users the BER performance achieves up to 10^{-6}. For single user the SNR is beyond -5 dB and for half loading (16 users) the SNR is beyond 7 dB. For full loading (32 users) the SNR is beyond 10 dB.

8.2 Performance of VSAT MC-CDMA system using convolutional code

The decoder type used for convolutional coding is the Viterbi decoder with code rate $R = \frac{1}{2}$.
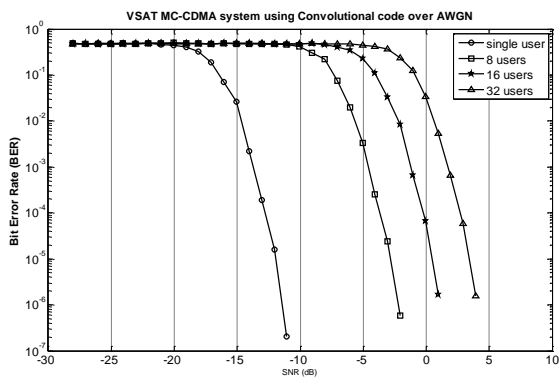

Fig.15 Performance of VSAT MC-CDMA system using Convolutional code (for single, 8, 16 and 32 users)

Figure 15 shows the performance of VSAT MC-CDMA system over AWGN channel for single, 8, 16 and 32 users. For single user the BER performance achieves up to 10^{-7} at SNR beyond -11 dB and for half loading (16 users) the BER performance achieves $1{,}65 . 10^{-6}$ at SNR beyond 1

dB. The BER performance achieves $1{,}54 . 10^{-6}$ at SNR beyond 4 dB for full loading (32 users).

8.3 Performance of VSAT MC-CDMA system using Turbo code

The decoder type used for Turbo coding is the Max-Log-Map with code rate $R = \frac{1}{3}$.
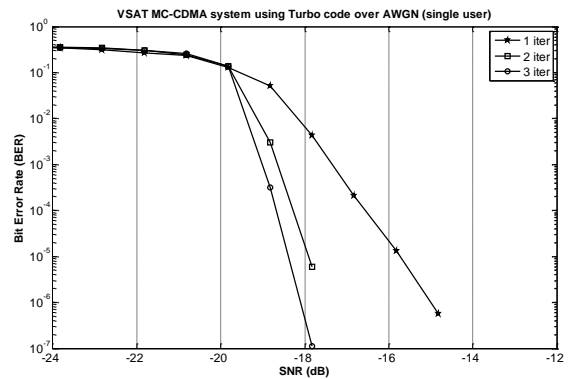

Fig.16 Performance of VSAT MC-CDMA system using Turbo code (For Single user)

Figure 16 shows the performance of VSAT communication link over AWGN channel for Single user. BER performance achieves 10^{-7} at SNR beyond -17,8 dB at 3th iteration. We stop at 3th iteration since there is no additional improvement in term of BER for further iterations.
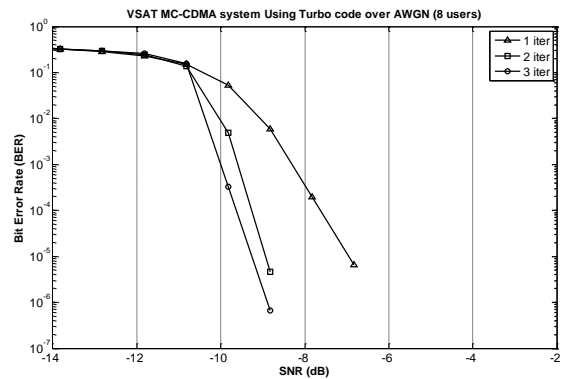

Fig.17 Performance of VSAT MC-CDMA system using Turbo code (for 8 users)

Figure 17 shows the performance of VSAT communication link over AWGN channel for 8 users. BER performance achieves up to 10^{-7} at SNR beyond -8,8 dB at 3th iteration.

Mohammed El Jourmi, Hassan El Ghazi,
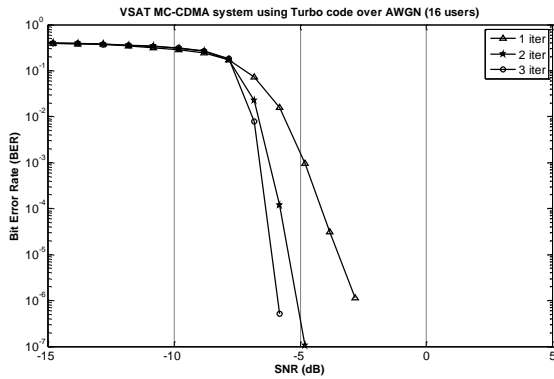Abdellatif Bennis, Hassan Ouahmane

Fig.18 Performance of VSAT MC-CDMA system
using Turbo code (for 17 users)

Figure 18 shows the performance of VSAT MC-CDMA system over AWGN channel for 16 users. at 3th iteration the BER performance achieves up to 10^{-7} at SNR beyond -5,8 dB.
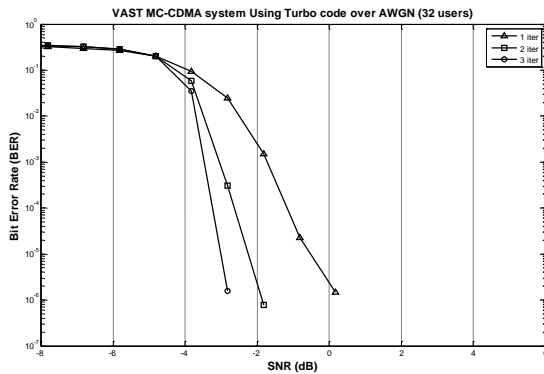

Fig.19 Performance of VSAT MC-CDMA system
using Turbo code (for 32 users)

Figure 19 shows the performance of VSAT MC-CDMA system over AWGN channel for 32 users, full loading. at 3th iteration the BER performance achieves up to 10^{-6} at SNR beyond -2,8 dB.
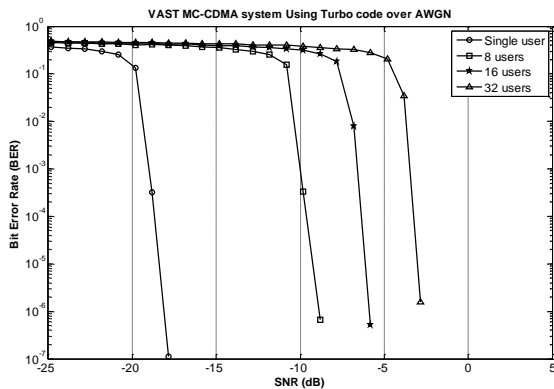

Fig.20 Performance comparison between single
user, 4 users, 16 users and 32 users (3th iteration)

Figure 20 shows the performance of VSAT MC-CDMA system for different amount of loading. Depending upon the number of active users, amount of loading, the link performance degrades gradually. But there is less performance degrading from half loading (16 users) to full loading (32 users) compared with the results from minimum loading (single user) to half loading (16 users).

Conclusion

In this paper, the performance of VSAT MC-CDMA system has been investigated by using the most popular type of multiple access technique, Code Division Multiple Access (CDMA) combining with multicarrier transmission system. To get the lower bit error rate, the most common types of channel coding methods (Turbo Coding and convolutional coding) are used. The results show that the performance depends upon the number of active users in the network.

In conclusion, the performance of VSAT MC-CDMA system coded with turbo code was better than the coded system with convolutional code.

References:
[1] Jonathon, Y., C. Cheah, M.E. Davis, "*Tone Interference in VSAT Sptectrum,*" IEEE Transactions on Communications, Vol. 45, No. 9, pp. 1035-1038, September 1997.
[2] A. J. Viterbi, *CDMA: Principles of Spread Spectrum Communication*. Addison-Wesley Publishing Company,1995.
[3] R. Prasad, *CDMA for Wireless Personal Communications*. Artech House, Inc., 1996.
[4] S. G. Glisic and P. A. Lepp̈annen, *Wireless Communications TDMA versus CDMA*. Kluwer Academic Publishers,1997.
[5] Rappaport, T.S., *Wireless Communications, 2nd ed*., Prentice Hall, 2002.
[6] Kamil,Sh. Zigangirov. *Theory of Code Division Multiple Access Communication*.Institute of Electrical and Electronics Engineers,2004.
[7] H. E. Ghazi, "*Allocation Algorithm for Optimizing MC-CDMA Over Correlated Channel*"accepted by WSEAS Trans. On commun.2010.
[8] Q. Shi and M. Latva-Aho, "*Performance analysis of MC-CDMA in Rayleigh fading channels with correlated envelopes and phases,*" IEE Proc. Commun., vol. 150, pp. 214–220, June 2003.

[9] Maral, G. 1996. *VSAT Networks*. New York: John Wiley & Sons Ltd.

[10] John Wiley & Sons Ltd, The Atrium, Southern Gate, Chichester, West Sussex PO19 8SQ, England. *Theory and Applications of OFDM and CDMA Wideband Wireless Communications, 2005*.

[11] Evans, B.G., *Satellite Communication Systems, 3rd ed.*, United Kingdom. The Institution of Electrical Engineers, 1999.

[12] Elbert, B.R., *The Satellite Communication Ground Segment and Earth Station Handbook,* Artech House, 2000.

[13] Elbert, B.R., *Introduction to Satellite Communication 3rd* , Artech House, 2008.

[14] Moheb, H., C. Robinson, J. Kijeski, "*Design and Development of Co-Polarized Ku-band Ground Terminal System for VSAT Application,*" IEEE Publications 0-7803-5639-X/99, pp. 2158-2161, 1999.

[15] R. zayani, S. Zid, R. Bouallegue, « *Simulateur des non-linéarités HPA sur un système OFDM* » OHD Conference, septembre 2005.

[16] A. N. D'Andrea, V. Lottici and R. Reggiannin, «*Nonlinear Predistortion of OFDM Signals over Frequency-Selective Fading Channels*», IEEE Transactions on Communications. Vol. 49. N° 5. pp. 837-843. 2001.

[17] G. L. Stuber, *Principles of Mobile Communications*. Kluwer Academic Publishers,1996.

[18] W. C. Jakes, *Microwave Mobile Communications*. IEEE Press, 1974.

[19] J. Cavers, *Mobile Channel Characteristics*. Kluwer Academic Publishers, 2000.

[20] F. Adachi, D. Garg, S. Takaoka, and K. Takeda, *"Broadband CDMA techniques," IEEE Wireless Communications*, vol. 12, no. 2, pp. 8–1/8, April 2005.

[21] R. V. Nee and R. Prasad, *OFDM For Wireless Multimedia Communications*. Artech House, 2000.

[22] *3GPP, \3GPP TS 45.003 V7.5.0."* Internet, 2008.

[23] C. Berrou, A. Galvieux, and P. Thitimajshima, "*Near Shannon limit error-correcting coding and decoding: Turbo-codes*," in Proc. 1993 IEEE Int. Conf. Commun., Geneva, Switzerland, 1993, vol. 2, pp. 1064–1070.

[24] B. Sklar, Digital Communications: Fundamentals and Applications. *Second ed. Fundamentals of Turbo Codes*. 2001: Prentice Hall.